Finline and Metal Insert Filters with Improved Passband Separation and Increased Stopband Attenuation

RUEDIGER VAHLDIECK, MEMBER, IEEE, AND WOLFGANG J. R. HOEFER, SENIOR MEMBER, IEEE

Abstract—A new class of optimized finline and metal insert filters is introduced. In these filters, the ladder-type insert is located in a waveguide section which is either wider or narrower than the embedding standard waveguide. A step junction at each end forms the transition to the standard waveguide and is included in the analysis. Both filter types provide a better suppression of spurious passbands and have significantly improved stopband attenuation. Filters with enlarged sections are useful for design at the lower end of the waveguide band, whereas the narrower version is appropriate for bandend design.

I. Introduction

MILLIMETER-WAVE applications of conventional finline and metal insert filters have drawn considerable attention over the past few years [1]–[12]. These filters consist of ladder-type inserts centered in the E-plane of rectangular waveguides (Fig. 1(a)). The inserts are easily fabricated with photolithographic techniques, and since a rigorous and general computer program for optimized design and analysis of such structures has been developed [3]–[5], their geometry can be predicted with high accuracy. This is so because the generalized scattering matrix formulation of the filter problem includes a large number of higher order modes and takes the finite metallization thickness into account. The method has been applied successfully to both narrow-band and broad-band filter designs up to 140 GHz.

In both applications, these filters perform well when the passband is centered within the operating band of the waveguide (Fig. 1(a)). However, their performance deteriorates when they operate either at the lower or at the higher end of the waveguide band. In the first case, the harmonic passband can fall within the single-mode range of the waveguide (Fig. 1(b), curve 1). In the second case, the stopband attenuation is reduced significantly towards higher frequencies (Fig. 1(b), curve 2). The reason for both phenomena is quite different and, to the knowledge of the authors, has not yet been discussed in detail in the literature.

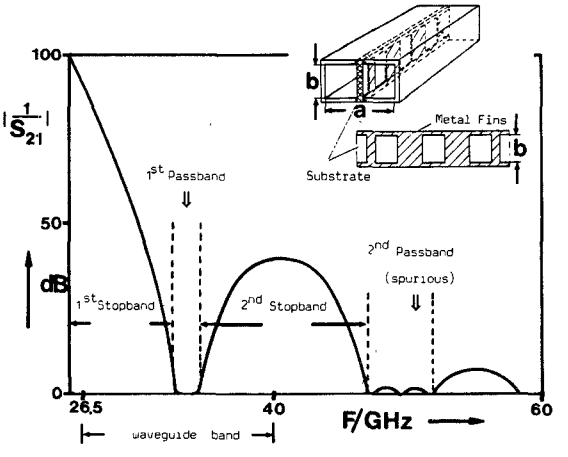

Fig. 1. (a) Conventional three-resonator finline filter with low dielectric permittivity ($\epsilon_r = 2.22$). The passband is situated in the middle of the single-mode range of the waveguide. (b) Conventional four-resonator single metal insert filter designed for the lower end (curve 1) or higher end (curve 2) of the waveguide band. The metal inserts have thickness of 150 μm.

II. Problems Associated with Conventional E-Plane Filter Design

Filters for the lower end of the waveguide band have rather long resonators because of the rapid increase of the guided wavelength toward cutoff. Therefore, their harmonic resonance can occur within the single-mode range of the guide. Moreover, because of the high waveguide attenuation close to cutoff, the resonators are relatively lossy.

Manuscript received March 22, 1985; revised July 11, 1985. This work was supported in part by the National Science and Engineering Research Council of Canada.

The authors are with the Department of Electrical Engineering, University of Ottawa, Ottawa, Ontario, Canada K1N 6N5.

0018-9480/85/1200-1333$01.00 ©1985 IEEE

TABLE I

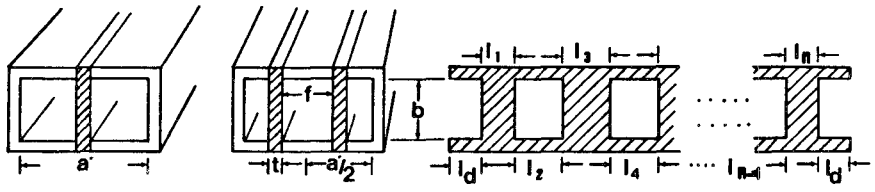

Standard waveguide dimension mm	Insert type	Narrower waveguide section mm	Enlarged waveguide section mm	Number of resonators	t μm	l_d mm	$l_1=l_n$ mm	$l_2=l_{n-1}$ mm	$l_3=l_{n-2}$ mm	$l_4=l_{n-3}$ mm	$l_5=l_{n-4}$ mm	l_6	Fig.
Ka-band a=7.112 b=3.556	Single metal insert	a=5.689 b=3.556		4	50.	0.	0.984	3.884	3.008	3.898	3.392		5 curve 2
	Twin metal insert		a'=7.8 b=3.556	5	50.	0.2	0.25	6.708	1.708	6.821	1.946	6.826	6 curve 2

On the other hand, filters designed for the bandend have a poor second stopband attenuation because an increasing amount of power is carried by parasitic modes across the coupling sections between the septa and the waveguide walls [11], even before the onset of the second-harmonic passband. Indeed, one would expect that the filters become transparent as soon as parasitic modes start to propagate across the coupling sections, resulting in a genuine high-pass behavior. However, this does not occur; rather, a well-defined anomalous passband is usually observed between the regular passbands. It appears that this is due to a mismatch between the resonator and the coupling sections; only when the parasitic mode wavelength becomes commensurate with the length of the coupling sections, series-type resonances occur, resulting in a total transmission and, hence, anomalous passband. This phenomenon is illustrated in Fig. 2, which shows the transmission characteristic of a single coupling section for (a) long and (b) short septa versus the frequency. The long septa produce strong periodic H_{10} transmission peaks ($|S_{21}|=1.$) which coincide with resonances of the first propagating mode (H'_{10}) in the coupling regions. The magnitude of evanescent higher order modes excited in the output waveguide (H_{30}, H_{50}) show the same frequency dependence.

For short septa, coupling resonances occur at much higher frequencies. Furthermore, transmission minima are less pronounced, indicating a growing contribution of higher order modes to the transfer of energy across the coupling section. Fig. 2(c) clearly shows the existence of an anomalous passband due to these resonances in the coupling sections of a finline filter. The correlation between coupling resonances and anomalous passbands is obvious.

III. Realization of the New Filters

To alleviate the latter problem, three different solutions have been proposed previously:

1) increase the thickness of the metal insert [5];
2) use a narrower waveguide for the filter section which is matched to the standard waveguide with a taper at each end [11];
3) use a twin metal insert rather than a single one [7].

The first two solutions require precision machining and are, therefore, no longer realizable with low-cost techniques. Furthermore, the addition of a taper section increases the length of the filter component. The third solution requires a greater effort in the mounting and adjustment of the twin metal inserts in the waveguide mount. The present paper proposes a fourth solution which combines the advantages of the previous attempts without complicating the realization of the filter.

The main feature of this solution is to reduce the width of the filter section as in solution 2) in order to increase the attenuation of parasitic modes in the coupling subsections. The taper, however, is replaced by a single-step transition (see Fig. 3(b)). The effect of this inductive step is included in the filter analysis and optimization. The realization of such filters is straightforward because the narrower filter section can simply be inserted between two standard waveguide flanges.

The same design principle applies to the realization of filters for the lower end of the waveguide band. To reduce the length of the resonators (in order to increase the separation between the regular passbands) the filter section

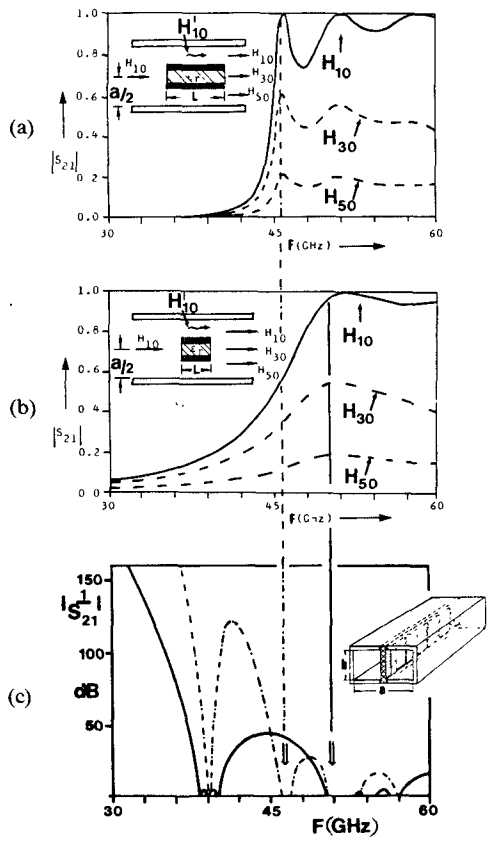

Fig. 2. Transmission coefficients S_{21} of dominant and next higher order modes when a H_{10} wave is incident in the coupling section of a finline filter. Waveguide dimensions: $a = 7.112$ mm, $b = a/2$, substrate thickness $D = 254$ μm, $\epsilon_r = 2.22$, metallization thickness $t = 17.5$ μm.

Length of the septa: (a) $l = 10$ mm, (b) $l = 4$ mm, (c) Not optimized four-resonator finline filter. The individual coupling sections have the same length: $l = 10$ mm (- · · · · · -) and $l = 4$ mm (———).

is widened such that the first passband is now centered in the single-mode range of that section. By inserting the filter section directly between two standard waveguide flanges (see Fig. 3(a)), we are able to increase the Q-factor, shorten the filter length, and push the spurious harmonic passband up in frequency without complicating the realization of the filter component. In this way, the essential advantages of these filters, namely high design accuracy and low-cost manufacturing, are preserved. Furthermore, the overall size of the filter is kept as short as possible.

IV. Theory

The theoretical treatment of the filter section has already been described in [3]–[5]; therefore, only the scattering matrix of the single-step transition will be explained in this paper.

The electromagnetic field in each subregion

$$\vec{E}^{(i)} = -j\omega\mu\nabla \times \vec{\Pi}_m^{(i)} \quad \vec{H}^{(i)} = \nabla\nabla \times \vec{\Pi}_m^{(i)} \tag{1}$$

can either be derived from the z-component (axial component) of the magnetic Hertz potential or from its x-component as has been shown in [3]–[5]. This is so because the transition to a narrower or wider waveguide section does

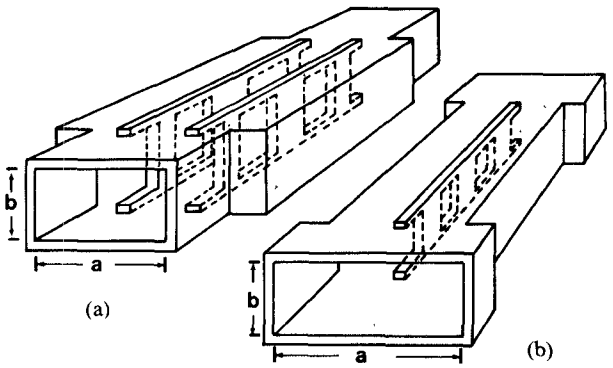

Fig. 3. The new filter design. (a) Twin metal insert filter in an enlarged waveguide section and (b) a single metal insert filter in a narrower waveguide section.

not contain any discontinuity in the y-direction ($\partial/\partial_y = 0$). Consequently, only TE_{n0}-waves are excited by a TE_{10}-wave, and only E_y, H_x, and H_z components will appear. In this paper, the electromagnetic field in each subregion is derived from the axial component of the magnetic Hertz vector $\vec{\Pi}_m = \vec{ez} \cdot \Pi_{mz}$, where Π_{mz} is expressed as the sum of orthogonal eigenfunctions

$$\Pi_{mz}^{(i)} = \sum_n T_{(n)}^{(i)} \cos kx_{(n)}^{(i)} \cdot p^{(i)} \left[r_{(n)}^{(i)+} e^{-jkz_{(n)}^{(i)} \cdot z} + r_{(n)}^{(i)-} e^{jkz_{(n)}^{(i)} \cdot z} \right] \tag{2}$$

with

$$kx_{(n)}^{(i)} = \frac{n \cdot \pi}{f^{(i)}}$$

$$f^{(i)\prime} = (a, c-d)$$

$$P^{(i)\prime} = (x, x-d)$$

and

$$T_{(n)}^{(i)} = \frac{1}{\sqrt{\omega\mu kx_{(n)}^{(i)2} \cdot S_F^{(i)}}}$$

$$S_F^{(2)} = \frac{(c-d)\cdot b}{2}$$

$$S_F^{(1)} = \frac{ab}{2}$$

$r_{(n)}^{(i)+}$ and $r_{(n)}^{(i)-}$ denote the amplitudes of the incident and reflected waves normalized to T so that the power which is transported by a given wave is 1 W. Since the transverse field components E_y and H_x must be continuous at the common interface $z = 0$, both amplitudes can be related to each other by the scattering matrix of the step junction (Fig. 4(a)) as follows:

$$\begin{bmatrix} r^{(1)-} \\ r^{(2)+} \end{bmatrix} = \underbrace{\begin{bmatrix} E & -L_E \\ L_H & E \end{bmatrix}^{-1} \cdot \begin{bmatrix} -E & L_E \\ L_H & E \end{bmatrix}}_{S_T} \cdot \begin{bmatrix} r^{(1)+} \\ r^{(2)-} \end{bmatrix} \tag{3}$$

TABLE II

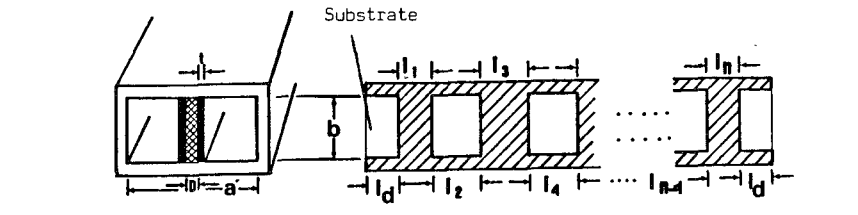

Standard waveguide dimensions mm	Narrower waveguide section	Number of resonators	Substr. thickness µm	ϵ_r	t µm	l_d mm	$l_1=l_n$ mm	$l_2=l_{n-1}$ mm	$l_3=l_{n-2}$ mm	$l_4=l_{n-3}$ mm	l_5 mm	Fig.
Ka-band a=7.112 b=3.556	a'=5.689 b =3.556	4	127.	2.22	10.	8.465	0.641	3.701	2.227	3.735	2.462	7 curve 2
K-band a=10.7 b=4.32	a'=8.2 b =4.32	4	254.	10.5	17.	5.94	0.091	5.771	1.381	5.958	1.718	8 curve 2

E denotes the unity matrix and L_E the submatrix

$$L_{E_{(mn)}} = \sqrt{4 \cdot kz_{(m)}^{(1)}/a \cdot (c-d) kz_{(n)}^{(2)}} \cdot F_s$$

L_H is the transposed matrix of L_E, $L_H = L_E^T$. F_s denotes the coupling matrix of the common interface [3]–[5]

$$F_{s_{(mn)}} = \int_d^c \cos kx_{(m)}^{(1)} x \cdot \cos kx_{(n)}^{(2)} (x-d)\, dx.$$

The scattering matrix of a step transition between a standard waveguide and the enlarged filter section is described in a similar way. The combination of the S-matrix of the step junction with either an air-filled waveguide section (S_a, see Fig. 4(b)) of finite length (for the metal insert filter) or a dielectric slab-loaded waveguide section of finite length (for the finline filter) makes the design procedure very flexible. The length of the filter mount can be fixed in advance, and the insert dimensions can then be optimized accordingly. Thus, one single housing is suitable for a large number of filters with different characteristics. This feature keeps production costs to a minimum.

Provided that the embedding waveguides have identical dimensions, the scattering matrix of the second step S_T' (back to the standard waveguide, see Fig. 4(b)) can simply be determined from the first one

$$S_T' = \begin{bmatrix} S_{T22} & S_{T21} \\ S_{T12} & S_{T11} \end{bmatrix}. \tag{4}$$

The scattering matrices of the individual coupling and resonator sections of finline and metal insert filters are already known, and the reader is referred to [3]–[5], [11] for detailed information.

The algorithm for obtaining the scattering matrix of the entire filter, including the step discontinuities, will be explained for a metal insert filter in a narrower waveguide section, but is similar in all other configurations. As a first step, we combine the scattering matrix of the step transition and of the first air-filled waveguide section into S_{j1}. Then, the scattering matrix of the first coupling section is combined with the former (S_{j1}) into S_{j2} which has the following submatrices:

$$S_{j2(11)} = S_{j1(11)} + S_{j1(12)} \cdot \left(E - S_{c1(11)} \cdot S_{j1(22)}\right)^{-1} \cdot S_{c1(11)} \cdot S_{j1(21)}$$

$$S_{j2(12)} = S_{j1(12)} \cdot \left(E - S_{c1(11)} \cdot S_{j1(22)}\right)^{-1} \cdot S_{c1(12)}$$

$$S_{j(21)} = S_{c1(21)} \cdot \left(E - S_{j1(22)} \cdot S_{c1(11)}\right)^{-1} \cdot S_{j1(21)}$$

$$S_{j2(22)} = S_{c1(22)} + S_{c1(21)} \left(E - S_{j1(22)} \cdot S_{c1(11)}\right)^{-1} \cdot S_{j1(22)} \cdot S_{c1(12)}$$

where E denotes the unity matrix. For the additional inclusion of the scattering matrix of the first resonator section, replace S_{j1} by S_{j2} and S_{c1} by S_{R1}. By repeating this algorithm, one finally obtains the total scattering matrix S_Σ of the entire filter component.

V. Results

All results presented in this paper have been obtained with a computer program which takes into account the finite thickness of metallization, up to 35 higher order modes and contains an optimization routine which has already been described in [3]–[5], but in addition permits the optimization of the return loss in the passband.

A. Metal Insert Filters

Fig. 5 compares a conventional single metal insert filter designed for the bandend (curve 1) with the new design featuring a narrower filter section (curve 2). The thickness of both inserts is 50 µm. Note the increased stopband attenuation and the shift of the anomalous passband towards 55 GHz. In these filters, propagation of parasitic modes along the coupling subsections is suppressed up to higher frequencies resulting in an improved stopband at-

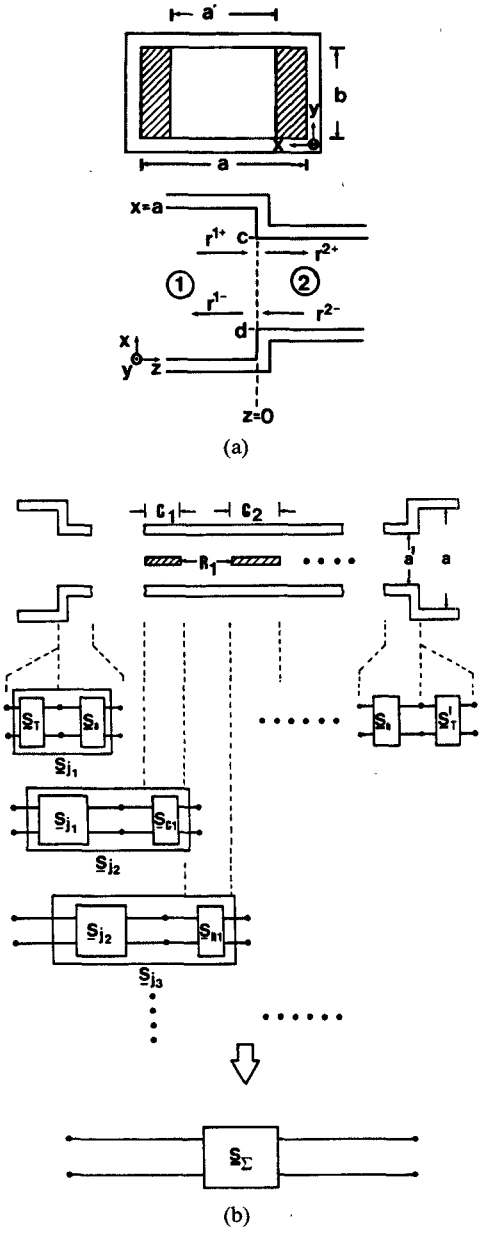

Fig. 4. (a) Step transition from a standard waveguide to a narrower waveguide section. (b) Block diagram showing the algorithm to obtain the scattering matrix of the entire filter component S_Σ by a suitable combination of the individual scattering matrices.

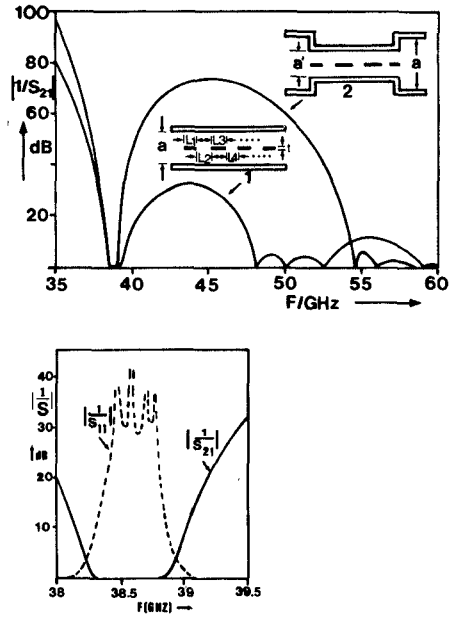

Fig. 5. Four-resonator single metal insert filters. Standard waveguide dimensions $a = 7.112$ mm, $b = a/2$. Curve 1: conventional filter type, $t = 150$ μm; curve 2: the new design in a narrower waveguide, $a' = 5.689$ mm, $t = 50$ μm.

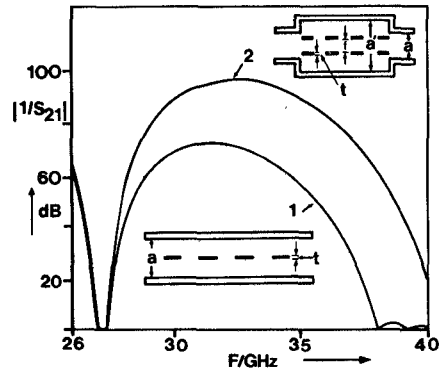

Fig. 6. Conventional four-resonator single metal insert filter designed for the lower end of the waveguide band (curve 1, $t = 100$ μm). Standard waveguide dimensions: $a = 7.112$ mm, $b = a/2$. Curve 2: Five-resonator twin metal insert filter in an enlarged waveguide section, $a' = 7.8$ mm, $t = 50$ μm.

tenuation which can be increased even more by further lowering the waveguide width. Then, however, the resonator length increases and the harmonic spurious passband decreases significantly.

This is the major problem facing the designer of conventional bandpass filters at the lower end of the waveguide band. At these frequencies the resonator length increases rapidly, causing a harmonic spurious passband within the single-mode range of the waveguide band.

By placing a single metal insert filter in an enlarged waveguide section, one can increase the separation between the regular passbands. At the same time, however, the anomalous passband effect occurs at lower frequencies because the width of the coupling subsections between the septum and the waveguide walls increases. To avoid this problem, we can use either a thicker single metal insert or a pair of thin metal inserts known as twin metal inserts [7].

Fig. 6 compares the transmission characteristic ($1/S_{21}$) of a twin metal insert filter in an enlarged waveguide section (curve 2) with a conventional single metal insert filter (curve 1). The spurious harmonic passband is pushed up in frequency, and the stopband attenuation is improved significantly.

B. Finline Filters

The design of finline filters for the bandend poses the same problems as that of single metal insert filters. Again, by reducing the width of the housing in the filter section,

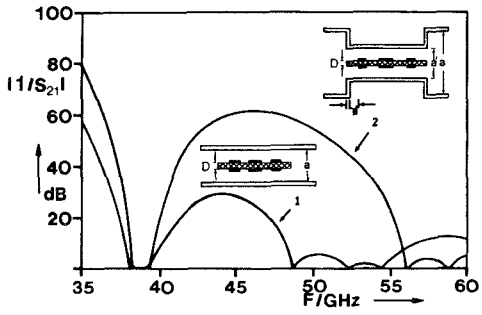

Fig. 7. Four-resonator finline filters. Standard waveguide dimensions $a = 7.112$ mm, $b = a/2$, substrate thickness: $D = 127$ μm, $\epsilon_r = 2.22$, $t = 10$ μm. Curve 1: conventional finline filter; curve 2: the new design in the narrower waveguide section, $a' = 5.689$ mm.

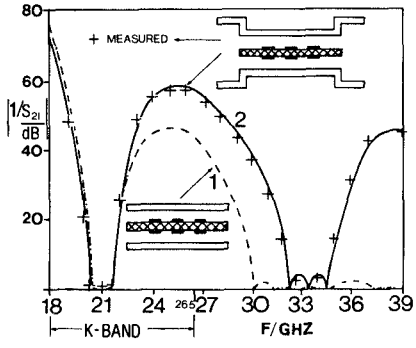

Fig. 8. Measured filter response of a K-band finline filter in a narrower waveguide section. Curve 1: conventional finline filter with low substrate permitivity ($\epsilon_r = 2.22$); curve 2: finline filter with a high substrate permittivity ($\epsilon_r = 10.5$) in a narrower waveguide section. $a = 10.7$ mm, $a' = 8.2$ mm, $b = 4.32$ mm, metallization thickness $t = 17.0$ μm, substrate thickness $D = 254$ μm.

we can increase the frequencies of both anomalous and harmonic spurious passbands. This measure widens the intermediate stopband and, at the same time, increase its attenuation. Fig. 7 compares the conventional finline filter (curve 1) with the new design in a narrower waveguide section (curve 2). The metallization thickness is 10 μm and the substrate material RT-Duroid ($\epsilon_r = 2.22$) has a thickness of 127 μm.

The design of finline filters for the lower end of the waveguide band can be improved in the same manner as that of metal insert filters. But in addition to broadening the waveguide in the filter region, the designer has the options of increasing either the substrate thickness or the substrate permittivity, or both. These options all lead to the same results: shorter resonator length, higher Q-factor, and broader second stopband with increased attenuation. Even for a filter application in the middle range of a waveguide band (for example, 21 GHz in the K-band (see Fig. 8)), the new filter design shows a better performance than the conventional finline filter which behaves as a genuine high-pass at frequencies above 30 GHz. However, the filter in the narrower waveguide section shows an improved second stopband and, furthermore, a distinct third stopband with a peak attenuation better than 40 dB at 39 GHz. The agreement between the theoretical prediction and the measured filter response is very good.

VI. Conclusion

A novel design approach for finline and metal insert filters has been introduced to improve characteristics at either the lower or higher extremeties of a waveguide band. Performance is improved by respectively widening or narrowing the waveguide in the filter section. The step transitions between the filter and the embedding standard waveguides are included in the analysis and optimization of the filters. By choosing steps rather than tapers, the ease and simplicity of fabrication of the filters are preserved, and the components are kept as short as possible. In comparison with their conventional counterparts, the new filters feature a better passband separation and higher stopband attenuation.

Acknowledgment

The filter described in Fig. 8 was realized and measured at COM DEV Ltd., of Cambridge, Ontario.

References

[1] Y. Tajima and Y. Sawayama, "Design and analysis of a waveguide-sandwich microwave filter," *IEEE Trans. Microwave Theory Tech.*, vol. MTT-22, pp. 839–841, Sept. 1974.

[2] Y. Konishi and K. Uenakada, "The design of a bandpass filter with inductive strip-planar circuit mounted in waveguide," *IEEE Trans. Microwave Theory Tech.*, vol. MTT-22, pp. 869–873, Oct. 1974.

[3] F. Arndt, J. Bornemann, D. Grauerholz, and R. Vahldieck, "Theory and design of low-insertion-loss finline filters," *IEEE Trans. Microwave Theory Tech.*, vol. MTT-30, pp. 155–163, Feb. 1982.

[4] J. Bornemann, R. Vahldieck, F. Arndt, and D. Grauerholz, "Optimized low-insertion-loss millimetre-wave fin-line and metal insert filters," *Radio Electron. Eng.*, vol. 52, no. 11/12, pp. 513–521, Nov./Dec. 1982.

[5] R. Vahldieck, J. Bornemann, F. Arndt, and D. Grauerholz, "Optimized waveguide E-plane metal insert filters for millimeter-wave applications," *IEEE Trans Microwave Theory Tech.*, vol. MTT-31, pp. 65–69, Jan. 1983.

[6] Y.-C. Shih and T. Itoh, "Computer-aided design of millimeter-wave E-plane filters," *IEEE Trans. Microwave Theory Tech.*, vol. MTT-31, pp. 135–141, Feb. 1983.

[7] J. Bornemann, F. Arndt, R. Vahldieck, and D. Grauerholz, "Double planar integrated millimeter-wave filter," in *13th Eur. Microwave Conf.* (Nuernberg, West Germany), Sept. 5–8, 1983, pp. 168–173.

[8] Y.-C. Shih and T. Itoh, "E-plane filters with finite-thickness septa," *IEEE Trans. Microwave Theory Tech.*, vol. MTT-31, pp. 1009–1012, Dec. 1983.

[9] R. Vahldieck, J. Bornemann, F. Arndt, and D. Grauerholz, "W-band low-insertion-loss E-plane filter," *IEEE Trans. Microwave Theory Tech.*, vol. MTT-32, pp. 133–135, Jan. 1984.

[10] Y.-C. Shih, "Design of waveguide E-plane filters with all metal inserts," *IEEE Trans Microwave Theory Tech.*, vol. MTT-32, pp. 695–704, July 1984.

[11] F. Arndt, J. Bornemann, R. Vahldieck, and D. Grauerholz, "E-plane integrated circuit filters with improved stopband attenuation," *IEEE Trans. Microwave Theory Tech.*, vol. MTT-32, pp. 1391–1394, Oct. 1984.

[12] L. Q. Bui, D. Ball, and T. Itoh, "Broad-band millimeter-wave E-plane bandpass filters," *IEEE Trans. Microwave Theory Tech.*, vol. MTT-32, pp. 1655–1658, Dec. 1984.

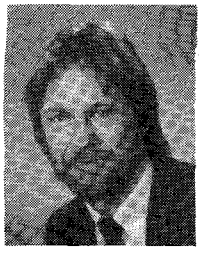

Rüdiger Vahldieck (M'85) was born in Heiligenhafen, West Germany, in 1951. He received the Dipl.-Ing. and the Dr.-Ing. degrees, both in electrical engineering, from the University of Bremen, Bremen, West Germany, in 1980 and 1983, respectively. His Dr.-Ing. thesis was on the numerical analysis of generalized finline configurations and the design and development of low insertion loss finline filters.

From 1980–1983, he was a Research Assistant at the Microwave Department of the University of Bremen, where he was engaged in computer-aided design of millimeter-wave integrated circuits. Since 1984, he has been a post-doctoral fellow at the University of Ottawa, Ottawa, Canada. His research activities at present have been chiefly concerned with broad-band millimeter-wave couplers and different numerical techniques to solve electromagnetic field problems in finline structures.

Dr. Vahldieck is one of the recipients of the A. F. Bulgin Premium of the Institution of Electronic and Radio Engineers, 1983.

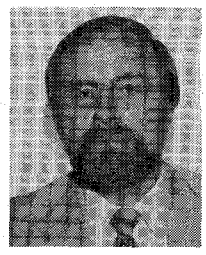

Wolfgang J. R. Hoefer (M'71–SM'78) was born in Urmitz/Rhein, Germany, on February 6, 1941. He received the diploma in electrical engineering from the Technische Hochschule Aachen, West Germany, in 1964, and the D.-Ing. degree from the University of Grenoble, France, in 1968.

After one year of teaching and research at the Institut Universitaire de Technologie, Grenoble, he joined the Department of Electrical Engineering, the University of Ottawa, Canada, where he is currently a professor. His sabbatical activities included six months with the Space Division of the AEG-Telefunken in Backnang, West Germany, in 1976, six months with the Institut National Polytechnique de Grenoble, France, in 1977, and one year with the Space Electronics Directorate, Communications Research Centre in Ottawa, Canada, during 1984/85. His research interests include microwave and millimeter-wave circuit design, numerical techniques for solving electromagnetic field problems, and microwave measurement techniques.

Dr. Hoefer is a registered Professional Engineer in the Province of Ontario, Canada.